Theoretical Study of the Interaction of Fe^+ with Silene

Jerzy Moc† and Mark S. Gordon*

Department of Chemistry, Iowa State University, Ames, Iowa 50011

Received July 18, 1996⊗

The reaction between Fe^+ in the ground ^6D and excited ^4F states and silaethylene have been studied using multiconfigurational (CASSCF) wave functions and multiconfigurational wave functions augmented by second-order perturbation theory (CASPT2), with basis sets of valence triple-ζ plus polarization quality. The open $H_2Si{-}CH_2Fe^+$ ($^6A'$)/cyclic ($H_2Si{-}CH_2$)-Fe^+ ($^4A''$) and the methyl structure $FeHSi{-}CH_3^+$ ($^6A''$, $^4A''$) isomers are found to be the most stable $FeSiCH_4^+$ isomers. Therefore, these are the most likely candidates for the two distinguishable $FeSiCH_4^+$ species observed in the gas-phase mass-spectrometric experiments by Jacobson and co-workers. This conclusion is further supported by the computed barriers of 42−50 kcal/mol separating the relevant pairs of the $FeSiCH_4^+$ isomers, the magnitude of which is consistent with the experimental estimate. On the quartet surface the net isomerization barrier (relative to separated reactants) is zero, whereas there is a net 7.2 kcal/mol barrier on the higher energy sextet surface.

Downloaded by CARLI CONSORTIUM on June 30, 2009
Published on January 7, 1997 on http://pubs.acs.org | doi: 10.1021/om960601s

I. Introduction

Gas-phase ion techniques have been a very useful tool for generation and characterization of reactive transition metal species.[1] For instance, studies of the reactions of atomic transition-metal ions with hydrocarbons in the gas phase have provided insight into the mechanism and energetics of such reactions.[2] The reactions of the Ti^+, V^+, Cr^+, Fe^+, Co^+, and Ni^+ ions with methylsilanes have recently been reported.[3]

Very recently, iron cationic $FeSiCH_4^+$ species have been generated and characterized in a series of gas-phase Fourier transform mass-spectrometric (FTMS) experiments by Jacobson and co-workers.[4,5] The nature of the $FeSiCH_4^+$ cations generated in these experiments was examined by methods such as collision-activated dissociation (CAD) and ion/molecule reactions, including isotopic exchange reactions. On the basis of the FTMS experiments,[4,5] the existence of two distinguishable and stable isomers of the $FeSiCH_4^+$ cation was inferred, and the formation of an iron−silene ($Fe^+{:}CH_2{=}SiH_2$) and an iron−silylene ($Fe^+{:}CH_3SiH$) species was suggested. Another important conclusion drawn by Jacobson and co-workers[4,5] was that no rearrangement between the two $FeSiCH_4^+$ isomers occurred under the experimental conditions. An implication of this observation was the existence of a high energetic barrier of *ca.* 40 kcal/mol separating the two isomeric forms of $FeSiCH_4^+$. Note that this estimate of the barrier height coincides with the magnitude of the barrier predicted earlier for the unimolecular rearrangement of the singlet silene H_2SiCH_2 to the singlet methylsilylene $HSiCH_3$ isomer of $SiCH_4$ (*vide infra*).

In the light of the ongoing gas-phase experiments of Jacobson and co-workers[4,5] we have undertaken a theoretical *ab initio* study of the reaction of Fe^+ with H_2SiCH_2 leading to the formation of the $FeSiCH_4^+$ products. Several questions are of interest here:

(1) What are the actual molecular structures of the two isomers of $FeSiCH_4^+$ observed experimentally? The experimental techniques mentioned above could only distinguish between them but provided no structural parameters.

(2) What are the relative energies of the two distinguishable $FeSiCH_4^+$ isomers and the transition state connecting them, i.e., the species involved in the interconversion process. These theoretical data will make it possible to estimate the barrier height associated with the isomerization in question. The experimental estimate[4,5] of the barrier is only approximate; thus, sophisticated *ab initio* electronic structure methods such as those used in the present work, and described below, should provide valuable insights.

(3) What is (are) the low-energy pathway(s) for the $Fe^+ + H_2SiCH_2$ reaction, resulting in the formation of the stable $FeSiCH_4^+$ cations?

(4) What is (are) the spin state(s) of the $FeSiCH_4^+$ products? There is no experimental information concerning the spin state for the observed $FeSiCH_4^+$ species. Due to the extremely small energy separation between the ground electronic state of Fe^+ (^6D) and its first excited state (^4F) (*vide infra*), one has to explore both the high-spin sextet and the low-spin quartet potential energy surfaces for the reaction of Fe^+ with H_2SiCH_2. We are not aware of any previous theoretical studies on the reaction of silene with transition metal cations.

II. Theoretical Methods and Computational Details

Three levels of theory were employed here, differing in the quality of the basis sets used and the electron correlation method applied. All structures were verified to be minima or

† Permanent address: Faculty of Chemistry, Wroclaw University, F. Joliot-Curie 14, 50-383 Wroclaw, Poland.

⊗ Abstract published in *Advance ACS Abstracts,* December 15, 1996.

(1) *Gas Phase Inorganic Chemistry*; Russell, D. H., Ed.; Plenum Press: New York, 1989.

(2) (a) Eller, K.; Schwarz, H. *Chem. Rev.* **1991**, *91*, 1121. (b) Armentrout, P. B. *Annu. Rev. Phys. Chem.* **1990**, *41*, 313. (c) Armentrout, P. B.; Beauchamp, J. L. *Acc. Chem. Res.* **1989**, *22*, 315.

(3) Kang, H.; Jacobson, D. B.; Shin, S. K.; Beauchamp, J. L.; Bowers, M. T. *J. Am. Chem. Soc.* **1986**, *108*, 5668.

(4) Bakhtiar, R.; Holznagel, C. M.; Jacobson, D. B. *J. Am. Chem. Soc.* **1993**, *115*, 345.

(5) Jacobson, D. B.; Bakhtiar, R. *J. Am. Chem. Soc.* **1993**, *115*, 10830.

S0276-7333(96)00601-2 CCC: $14.00 © 1997 American Chemical Society

Table 1. Active Spaces Employed in the CASSCF Calculations

species	state	orbitals included[a]	size[b]	no. of CSF's[c]
Fe^+	^6D	five Fe(3d), Fe(4s)	(7/6)	3
Fe^+	^4F	five Fe(3d), Fe(4s)	(7/6)	18
H_2SiCH_2	$^1A_1$	σ(Si−C), σ*(Si−C), π(Si−C), π*(Si−C)	(4/4)	12
$HSiCH_3$	$^1A'$	σ(Si−C), σ*(Si−C), lone pair on Si, empty Si(p_z)	(4/4)	12
$Fe^+\cdots H_2SiCH_2$ complex	$^6A'$	σ(Si−C), σ*(Si−C), π(Si−C), π*(Si−C), five Fe(3d), Fe(4s)	(11/10)	2490 (4950)
	$^6A''$		(11/10)	2460 (4950)
$Fe^+\cdots H_2SiCH_2$ complex	$^4A'$	σ(Si−C), σ*(Si−C), π(Si−C), π*(Si−C), five Fe(3d), Fe(4s)	(11/10)	9880 (19 800)
	$^4A''$		(11/10)	9920 (19 800)
$H_2Si-CH_2Fe^+$ open[d,e]	$^6A'$	σ(Si−C), σ*(Si−C), σ(C−Fe), σ*(C−Fe), five Fe(3d), Si(p_y)	(11/10)	2488 (4950)
	$^6A''$		(11/10)	2462 (4950)
$(H_2Si-CH_2)Fe^+$ cyclic[d,f]	$^4A'$	σ(Si−C), σ*(Si−C), σ(C−Fe), σ*(C−Fe), σ(Si-Fe), σ*(Si-Fe), four Fe(3d)	(11/10)	9792 (19 800)
	$^4A''$		(11/10)	10008 (19 800)
$FeHSi-CH_3^+$ methyl structure[d,e]	$^6A'$	σ(Si−C), σ*(Si−C), σ(Si−Fe), σ*(Si−Fe), five Fe(3d), Si(p_z)	(11/10)	2493 (4950)
	$^6A''$		(11/10)	2457 (4950)
$FeHSi-CH_3^+$ methyl structure[d,e]	$^4A'$	σ(Si−C), σ*(Si−C), σ(Si−Fe), σ*(Si−Fe), five Fe(3d), Si(p_z)	(11/10)	9832 (19 800)
	$^4A''$		(11/10)	9968 (19 800)
transition state (TS)[g]	^6A	σ(Si−C), σ*(Si−C), σ(Si−Fe), σ*(Si−Fe), five Fe(3d), Si(p_z)	(11/10)	4950
transition state (TS)[g]	^4A	σ(Si−C), σ*(Si−C), σ(Si−Fe), σ*(Si−Fe), five Fe(3d), Si(p_z)	(11/10)	19 800

[a] The superscript "*" indicates antibonding orbitals. [b] The first entry is the number of electrons, and the second entry is the number of orbitals in the active space. [c] The number of configuration state functions (CSF's) in the CASSCF wave function; within the parentheses is the number of CSF's under C_1 symmetry. [d] The *xy* plane is a symmetry plane. [e] Fe(4s) involved in the C−Fe bond. [f] Fe(4s) and one Fe(3d) involved in the C−Fe and Si−Fe bonds. [g] Fe(4s) involved in the Si−Fe bond.

Downloaded by CARLI CONSORTIUM on June 30, 2009
Published on January 7, 1997 on http://pubs.acs.org | doi: 10.1021/om960601s

transition states by calculating and diagonalizing the matrix of energy second derivatives (hessian).

A. Preliminary SCF Calculations. An initial mapping of the potential surface of the $FeSiCH_4^+$ ion was accomplished using the unrestricted Hartree−Fock (UHF) method. The calculations made use of the effective-core potentials (ECP) of Hay and Wadt[6] for the Fe and Si atoms, so only their outermost electrons were treated explicitly. These include electrons in the 3d and 4s orbitals for Fe and electrons in the 3s and 3p orbitals for Si, which were described by the associated basis sets of the form (3s2p5d)/[2s2p2d] and (3s3p)/[2s2p], respectively.[6] For C and H, the all-electron Dunning−Huzinaga double-ζ bases of the form (9s5p)/[3s2p] and (4s)/[2s], respectively, were utilized.[7,8] Henceforth, we will refer to the resulting ECP and basis set combination as ECPDZV. The structures were gradient optimized within the appropriate symmetry, followed by single point calculations using the second-order Møller−Plesset (MP2)[9] perturbation theory with spin projection (PMP2).[10] To ensure that the electronic configuration leading to the lowest PMP2/ECPDZV energy was chosen, geometry optimizations with several alternate occupations of the starting molecular orbitals were performed for each structure. The UHF-based calculations were carried out with GAUSSIAN92.[11]

B. CASSCF Geometry Optimizations. On the basis of the preliminary explorations of the potential energy surfaces described above, selected portions of the sextet and quartet surfaces for the reaction $Fe^+ + H_2SiCH_2$ were next explored using the complete active space self-consistent-field (CASSCF) multiconfigurational wave functions.[12] The ECPDZV basis set described above was utilized for this purpose. The CASSCF wave function accounts for near-degeneracy correlation effects, which are frequently important in compounds containing transition metals.[13] In the choice of the relevant active spaces, the molecular orbitals corresponding to bonds that are described adequately at the HF level and are not involved in the current step of the reaction were omitted.[14] The active spaces employed in the CASSCF calculations for the various species are indicated in Table 1. Note that the core carbon 1s atomic orbital was not correlated, since it is doubly occupied in every configuration state function (CSF). All the CASSCF/ECPDZV structure optimizations were carried out with the GAMESS code.[15]

C. CASSCF−CASPT2 Energy Calculations. The dynamic correlation effects were treated using multiconfigurational second-order perturbation theory, CASPT2,[16] in which a CASSCF type wave function is employed as a reference function. It has been suggested[17] that the CASPT2 method may be an effective alternative to the multireference configuration interaction (MRCI) technique, especially for larger systems.

All-electron valence triple-ζ plus polarization basis sets were utilized in the combined CASSCF−CASPT2 calculations to provide the final energetics. For Fe, we used the [10s6p] contraction of the (14s9p) primitive functions of Wachters[18] and the [3d] contraction of the (6d) primitive basis taken from the work of Rappé et al.[19] This basis set was supplemented with two sets of p functions ($\alpha = 0.231$ and $\alpha = 0.0899$).[15] The final basis set for Fe was of the form (14s11p6d)/[10s8p3d] and was used in conjunction with the polarized valence triple-ζ bases for the Si, C, and H atoms. For Si, this was the [6s5p] contraction derived by McLean and Chandler[20] from the (12s9p) primitive set[21] and supplemented with a single set of

(6) (a) Hay, P. J.; Wadt, W. R. *J. Chem. Phys.* **1985**, *82*, 270. (b) Wadt, W. R.; Hay, J. P. *J. Chem. Phys.* **1985**, *82*, 284.
(7) Dunning, T. H.; Hay, J. P. In *Modern Theoretical Chemistry*; Schaefer, H. F., III, Ed.; Plenum Press: New York, 1977; Vol. 3, pp 1−27.
(8) Huzinaga, S. *J. Chem. Phys.* **1965**, *42*, 1293.
(9) Pople, J.; Binkley, J. S.; Seeger, R. *Int. J. Quantum Chem. Symp.* **1976**, *10*, 1.
(10) Schlegel, H. B. *J. Chem. Phys.* **1986**, *84*, 4530.
(11) GAUSSIAN 92. Frisch, M. J.; Trucks, G. W.; Head-Gordon, M.; Gill, P. M. W.; Wong, M. W.; Foresman, J. B.; Johnson, B. G.; Schlegel, H. B.; Robb, M. A.; Replogle, E. S.; Gomperts, R.; Andres, J. L.; Raghavachari, K.; Binkley, J. S.; Gonzalez, C.; Martin, R. L.; Fox, D. J.; DeFrees, D. J.; Baker, J.; Stewart, J. J. P.; Pople, J. A. Gaussian, Inc., Pittsburgh, PA, 1992.
(12) For a review of the CASSCF method, see: Roos, B. O. In *Ab Initio Methods in Quantum Chemistry-II*; Lawley, K. P., Ed.; J. Wiley & Sons Ltd.: Chichester, U.K., 1987; pp 399−445.
(13) Roos, B. O. In *Lecture Notes in Quantum Chemistry;* Roos, B. O., Ed.; Springer: Berlin, 1992; Vol. 58, pp 175−254.
(14) Musaev, D. G.; Morokuma, K.; Koga, N.; Nguyen, K. A.; Gordon, M. S.; Cundari, T. R. *J. Phys. Chem.* **1993**, *97*, 11435.
(15) GAMESS (General Atomic and Molecular Electronic Structure System): Schmidt, M. W.; Baldridge, K. K.; Boatz, J. A.; Elbert, S. T.; Gordon, M. S.; Jensen, J. H.; Koseki, S.; Matsunaga, N.; Nguyen, K. A.; Su, S.; Windus, T. L.; Dupuis, M.; Montgomery, Jr., J. A. *J. Comput. Chem.* **1993**, *14*, 1347.
(16) (a) Andersson, K.; Malmqvist, P.-Å.; Roos, B. O.; Sadlej, A. J.; Wolinski, K. J. *J. Phys. Chem.* **1990**, *94*, 5483. (b) Andersson, K.; Malmqvist, P.-Å.; Roos, B. O. *J. Chem. Phys.* **1992**, *96*, 1218.
(17) (a) Andersson, K.; Roos, B. O. *Chem. Phys. Lett.* **1992**, *191*, 507 and references cited therein. (b) González-Luque, R.; Merchán, M.; Roos, B. O. *Chem. Phys.* **1993**, *171*, 107. (c) Pierloot, K.; Persson, B.; Roos, B. O. *J. Phys. Chem.* **1995**, *99*, 3465.
(18) Wachters, A. J. H. *J. Chem. Phys.* **1970**, *52*, 1033.
(19) Rappé, A. K.; Smedley, T. A.; Goddard, W. A., III. *J. Phys. Chem.* **1981**, *85*, 2607.
(20) McLean, A. D.; Chandler, G. S. *J. Chem. Phys.* **1980**, *72*, 5639.

d functions ($\alpha = 0.395$). For C, we used the [5s3p] contracted basis developed by Dunning[22] from the (10s6p) primitive functions[8] and augmented by a set of d functions ($\alpha = 0.72$). Similarly, for H, the [3s] basis derived[22] from the (5s) primitive set[8] and augmented by a set of p polarization functions ($\alpha = 1.0$) was utilized. Hereafter, the resulting basis will be referred to as TZV+P.

The CASSCF wave functions created with the TZV+P basis and employed as reference functions in the CASPT2 calculations were constructed in the same way as those using the ECPDZV basis. Here, the Ne core of Si and Ar core of Fe, as well as the carbon 1s orbital, were not correlated. The CASSCF−CASPT2 calculations were performed by means of the MOLCAS-2 package[23] and assuming the CASSCF/ECP-DZV structures.

III. Results and Discussion

The CASSCF-optimized structures of the singlet H_2SiCH_2 and $HSiCH_3$ isomers of $SiCH_4$ are depicted in Figure 1. Figures 2−4 show the CASSCF structures of the low-lying sextet and quartet states of the $FeSiCH_4^+$ species, and Figure 5 reveals the transition states involved in the isomerizations considered. Finally, the CASSCF and CASPT2 total and relative energies of $Fe^+(^6D)$, $Fe^+(^4F)$, H_2SiCH_2, $HSiCH_3$, and various $FeSiCH_4^+$ species, as computed using the TZV+P basis set, are reported in Tables 2−4.

A. Reactants. Closed-shell singlet silaethylene H_2SiCH_2 and methylsilylene $HSiCH_3$ have been proposed[24,25] to be the most stable isomers of $SiCH_4$. The two isomers have been the subject of considerable theoretical interest, focused on comparing their thermodynamic stabilities and estimating the magnitude of the barrier to the 1,2-hydrogen migration separating them.[24,25] The *ab initio* calculations conclude that singlet silaethylene and singlet methylsilylene lie close in energy. The best estimate of the respective energy difference is 3.6 kcal/mol, with silaethylene found to be more stable.[24b] There is a substantial 40 kcal/mol energy barrier to the 1,2-hydrogen shift from silaethylene to methylsilylene.[24fgh,29]

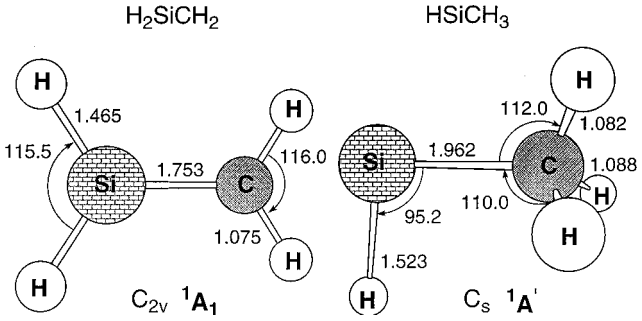

Figure 1. CASSCF (4/4) optimized geometries of silaethylene H_2SiCH_2 and methylsilylene $HSiCH_3$ (bond lengths in Å, bond angles in deg). In H_2SiCH_2, the *xz* plane is the plane of the molecule; in $HSiCH_3$, the symmetry plane is *xy*.

Our CASSCF-optimized structures of silaethylene and methylsilylene (Figure 1) agree well with those computed earlier using comparable basis sets;[24f] the main difference is longer Si−C bonds in the CASSCF structures due to the contribution from the antibonding orbitals to the wave function. The Si−C bond in methylsilylene is substantially longer than its silaethylene counterpart, by 0.21 Å, due to the stronger (double) bond in silaethylene. The relatively long Si−H bond in $HSiCH_3$ (1.523 Å) is similar to that in the parent SiH_2 ($^1A_1$) as computed with the comparable basis set.[35] In accordance with the previous theoretical studies,[24,25] the CASSCF−CASPT2 energy calculations reveal that the two $SiCH_4$ isomers are very close in thermodynamic stability. The CASSCF energy separation of 7.0 kcal/mol drops to 1.1 kcal/mol at CASPT2, with H_2SiCH_2 found again to be the more stable isomer (Table 2). Thus, the CASSCF and CASPT2 energy differences bracket the value of 3.6 kcal/mol derived from the high-quality single-configuration-based *ab initio* calculations.[24b]

It is known from experiment[26] that the second reactant, Fe^+, has a ^6D ($4s3d^6$) ground electronic state, with the first excited state, ^4F ($3d^7$), lying only 5.3 kcal/mol higher in energy.

Our CASSCF calculations (Table 2) predict the correct order of the two states, but the corresponding $^6D-^4F$ splitting of 37.9 kcal/mol is only slightly less than the ROHF value of 38.7 kcal/mol.[33] This is due to the modest configurational mixing at this level of theory and

Downloaded by CARLI CONSORTIUM on June 30, 2009
Published on January 7, 1997 on http://pubs.acs.org | doi: 10.1021/om960601s

(21) Huzinaga, S. Approximate Atomic wave functions. II. Department of Chemistry Report, University of Alberta, Edmonton, Alberta, Canada 1971.
(22) Dunning, T. H. *J. Chem. Phys.* **1971**, *55*, 716.
(23) Andersson, K.; Fülscher, M. P.; Lindh, R.; Malmqvist, P.-Å.; Olsen, J.; Roos, B. O.; Sadlej, A. J.; Widmark, P.-O. MOLCAS Version 2, User's Guide; University of Lund, Sweden, 1991.
(24) (a) Allendorf, M.; Melius, C. *J. Phys. Chem.* **1992**, *96*, 428. (b) Grev, R. S.; Scuseria, G. E.; Scheiner, A. C.; Schaefer, H. F., III; Gordon, M. S. *J. Am. Chem. Soc.* **1988**, *110*, 7337. (c) Luke, B. T.; Pople, J. A.; Krogh-Jesperson, M. B.; Apeloig, Y.; Karmi, M.; Chandrasekhar, J.; Schleyer, P. v. R. *J. Am. Chem. Soc.* **1986**, *108*, 270. (d) Luke, B. T.; Pople, J. A.; Krogh-Jesperson, M. B.; Apeloig, Y.; Chandrasekhar, J.; Schleyer, P. v. R. *J. Am. Chem. Soc.* **1985**, *107*, 537. (e) Gordon, M. S.; Truong, T. N. *Chem. Phys. Lett.* **1987**, *142*, 110. (f) Goddard, J. D.; Yoshioka, Y.; Schaefer, H. F., III. *J. Am. Chem. Soc.* **1980**, *102*, 7644. (g) Yoshioka, Y.; Schaefer, H. F., III. *J. Am. Chem. Soc.* **1981**, *103*, 7366. (h) Kohler, H. J.; Lischka, H. *J. Am. Chem. Soc.* **1982**, *104*, 5884.
(25) Gordon, M. S.; Francisco, J. S.; Schlegel, H. B. In *Advances in Silicon Chemistry;* JAI Press: Greenwich, CT, 1993; Vol. 2, pp 137−185 and references cited therein. For a list of *ab initio* papers on the silaethylene and methylsilylene prior to 1980, see ref 24f.
(26) Atomic Energy Levels of the Iron-Period Elements: Potassium through Nickel. Sugar, J.; Corioliss, C. *J. Phys. Chem. Ref. Data Suppl. 2* **1985**, *14*, 407−512.
(27) (a) Bauschlicher, C. W.; Langhoff, S. R.; Partridge, H.; Barnes, L. A. *J. Chem. Phys.* **1989**, *91*, 2399. (b) Sodupe, M.; Lluch, J. M.; Oliva, A.; Illas, F.; Rubio, J. *J. Chem. Phys.* **1989**, *90*, 6436 and references cited therein. (c) Bauschlicher, C. W.; Siegbahn, P.; Pettersson, L. G. M. *Theor. Chim. Acta* **1988**, *74*, 479. (d) Bauschlicher, C. W. *J. Chem. Phys.* **1987**, *86*, 5591.
(28) See, e.g.: Raghavachari, K.; Trucks, G. W. *J. Chem. Phys.* **1989**, *91*, 1062.
(29) Moc, J.; Nguyen, K. A.; Gordon, M. S. Submitted for publication.
(30) Sodupe, M.; Bauschlicher, C. W.; Langhoff, S. R.; Partridge, H. *J. Phys. Chem.* **1992**, *96*, 2118.
(31) Glaesemann, K.; Gordon, M. S. Unpublished results.
(32) (a) Sodupe, M.; Bauschlicher, C. W. *J. Phys. Chem.* **1991**, *95*, 8640. It has been pointed out in this work that it is not always straightforward to differentiate between the electrostatic and covalent bonding based on the character of the wave function. Instead, geometrical changes of the ligand were suggested to be a proper identification of the type of bonding. Indeed, we have found from Mulliken population analysis (TZV+P basis) that the net iron charge is 0.7 for the two open and two cyclic structures. (b) Again, the Mulliken net iron charges are rather similar for the sextet and quartet methyl structures, being 0.6 and 0.6−0.7, respectively. (c) This can be compared with the net iron charges in the initial complexes of +0.9.
(33) The other Hartree−Fock estimates of this splitting reported in the literature are similar; the two recent values are 38.0 kcal/mol (Ricca, A.; Bauschlicher, C. W.; Rosi, M. *J. Phys. Chem.* **1994**, *98*, 9498) and 38.9 kcal/mol (Heinemann, C.; Schwarz, J.; Koch, W.; Schwarz, H. *J. Chem. Phys.* **1995**, *103*, 4551).
(34) It has been suggested that the relative weight of ω in different electronic states can be a measure of how balanced the calculation is. See, e.g.: Fülscher, M. P.; Andersson, K.; Roos, B. O. *J. Phys. Chem.* **1992**, *96*, 9204.
(35) Meadows, J. H.; Schaefer, H. F., III. *J. Am. Chem. Soc.* **1976**, *98*, 4383.

Table 2. Comparison of Total (in hartrees) and Relative (in kcal/mol) Energies of the $Fe^+(^6D)$ and $Fe^+(^4F)$ Terms and the H_2SiCH_2 ($^1A_1$) and $HSiCH_3$ ($^1A'$) Isomers of $SiCH_4$[a]

method	$Fe^+(^6D)$	$Fe^+(^4F)$
CASSCF	−1262.181 95 (0.0)	−1262.121 59 (37.9)
PT2F	−1262.579 08 (0.0)	−1262.579 14 (0.0)
CASSCF[b]	−1262.182 99 (0.0)	−1262.134 04 (30.7)
PT2F[b]	−1262.725 78 (0.0)	−1262.718 07 (4.8)
exp[c]	(0.0)	(5.3)
method	**H_2SiCH_2 ($^1A_1$)**	**$HSiCH_3$ ($^1A'$)**
CASSCF	−329.126 11 (0.0)	−329.115 00 (7.0)
PT2F	−329.471 38 (0.0)	−329.469 55 (1.1)
lit.[d]	(0.0)	(3.6)

[a] The relative energies are in parentheses; TZV+P basis set was used, unless specified otherwise. [b] Obtained using the TZV+P basis set augmented by a set of f functions. [c] Reference 26; averaged over *J* states. [d] From ref 24b.

not recovering the full dynamic correlation effects.[27c,d] Inclusion of the CASPT2 dynamic correlation with the TZV+P basis leads to an overshoot of these effects. The resulting splitting reduces to 0 kcal/mol; thus, the quartet is now overstabilized by 5.3 kcal/mol with respect to experiment (Table 2).

One CASSCF−CASPT2 calculation for both states of Fe^+ was performed with the TZV+P basis augmented by a set of f functions ($\alpha = 1.663$),[31] since the latter are known to be important in calculations of this type.[28] Unfortunately, the use of this "extended" iron basis was prohibitive in the CASSCF−CASPT2 calculations of the $FeSiCH_4^+$ quartet states. Inclusion of f functions reduces the $^6D-^4F$ separation by 7 kcal/mol at the CASSCF level. Adding the CASPT2 correlation with the "extended" basis leads to an absolute deviation from experiment by only 0.5 kcal/mol (Table 2). The reproduction of the $^6D-^4F$ separation for Fe^+ by *ab initio* MO methods is a challenging problem.[b,37,38] Large basis sets are required to reproduce the experimental splittings in the first-row transition metal neutrals or cations.[17a,27,28,33,37] Also, in the multiconfigurational wave function based calculations of the splitting, the use of large active spaces, especially including a second 3d shell, might be necessary.[17a,37] The recent estimates by Musaev and Morokuma[37] and Ricca et al.[33] are 7.5 and 8.3 kcal/mol as obtained at the MR−SDCI (with ECP) and CCSD(T) (all electron) levels, respectively. Thus, the very good agreement with experiment obtained here may be somewhat fortuitous.

B. Preliminary Mapping of the Potential Energy Surface of $FeSiCH_4^+$. Initially, an extensive mapping of the sextet and quartet potential energy surfaces of $FeSiCH_4^+$ was accomplished by using the methods described in subsection II.A. For this purpose, a number of geometrical structures of $FeSiCH_4^+$ were studied. The major goals of this preliminary study were to (i) establish the candidates for the $FeSiCH_4^+$ isomers observed experimentally[4,5] and (ii) provide the starting geometries for the multiconfiguration-based calculations specified in subsections II.B. and II.C. The isomers described in detail below in subsections III.D and III.E were by far the most stable $FeSiCH_4^+$ isomers found from the preliminary calculations for both sextet and quartet multiplicities.

C. Complexes. A plausible initial intermediate for the reaction of Fe^+ with silaethylene is the planar ion−molecule complex $Fe^+\cdots H_2SiCH_2$ (Figure 2). Bonding with the $Fe^+(^6D)$ and $Fe^+(^4F)$ states gives rise to the corresponding sextet $^6A'$ (**1a**) and $^6A''$ (**1b**) and quartet $^4A'$ (**2a**) and $^4A''$ (**2b**) states of $Fe^+\cdots H_2SiCH_2$, respectively. This complex arises from interaction of the metal cation with one of the Si−H bonds in H_2SiCH_2. The Si−H bonds are more polarizable than the C−H bonds,[29] and one expects the Si−H bond to be polarized such that H is at the negative end. This enhances the interaction with the positively charged cation.

The CASPT2 calculations predict the ground state of $Fe^+\cdots H_2SiCH_2$ to be a $^4A''$ (**2b**) state, stabilized by 10.6 kcal/mol with respect to isolated $Fe^+(^4F) + H_2SiCH_2$. On the sextet surface, the lowest $^6A'$ (**1a**) state of $Fe^+\cdots H_2SiCH_2$ lies 9.6 kcal/mol below separated $Fe^+(^6D) + H_2SiCH_2$. Note that the energy difference between the $^4A''$ (**2b**) and $^6A'$ (**1a**) states is only 1 kcal/mol, reflecting the small $^6D-^4F$ splitting of Fe^+ discussed above. The moderate strength of the complex is indicated by the modest elongation of the involved Si−H bond of about 0.05 Å relative to that in isolated silaethylene. Due to the s orbital occupancy of the ^6D state of Fe^+ and consequently more metal−ligand repulsion,[30] the H···Fe interaction distance is longer for the sextet (**1a**, and **1b**) structures (2.21 Å) than for the quartet (**2a**,**b**) structures (2.13 Å); the remaining geometrical parameters are identical for all states of $Fe^+\cdots H_2SiCH_2$. As for the Si^+ analogue,[29] the complex features a nearly linear Si−H···Fe arrangement.

D. Open and Cyclic Isomers. Starting from the $Fe^+\cdots H_2SiCH_2$ complex, migration of Fe^+ is possible leading to the formation of the $FeSiCH_4^+$ isomers with the metal ion lying in the C_s symmetry plane perpendicular to the H_2SiCH_2 moiety (Figure 3). Of course, the structures shown in Figure 3 may also be formed directly from the separated reactants. The molecular structure and the relative stability of the resulting isomers depend chiefly on the Fe^+ electronic state.

On each sextet surface, an open type isomer $H_2Si-CH_2Fe^+$ is formed. These open structures, $^6A'$ (**3a**) and $^6A''$ (**3b**), exhibit a long C−Fe distance of about 2.50 Å, a slightly elongated Si−C bond (by 0.02 Å with respect to isolated H_2SiCH_2), and a slight bending of the CH_2 moiety out of the original molecular plane. These findings suggest that the bonding in sextet $H_2Si-CH_2Fe^+$ is strongly electrostatic in origin,[32a] although there is clearly some covalent contribution, since the positive charge on Fe is now only +0.7.[32c] The CASPT2 calculations predict the lowest state of $H_2Si-CH_2Fe^+$ to be $^6A'$ (**3a**), lying 34.9 kcal/mol below the respective reactants $Fe^+(^6D) + H_2SiCH_2$, with the $^6A''$ (**3b**) state being only 0.1 kcal/mol less stable (Table 4).

In the quartet states, the $Fe^+-H_2SiCH_2$ repulsion is smaller (because the 4s orbital of the cation is empty);[30] thus, the Fe^+ interaction with the ligand is stronger. Here, insertion of Fe^+ into the π bond of silaethylene occurs to form a three-membered ring as in $^4A'$ (**4a**) and $^4A''$ (**4b**). In the resulting cyclic type isomer (H_2Si-CH_2)Fe^+, the C−Fe bond distance of 2.11−2.12 Å is

(36) Note that, for the open $H_2Si-CH_2Fe^+$ isomer, the $^6A'$ (3a) and $^6A''$ (3b) states are nearly degenerate, so the ordering of the two states may change with improving the theoretical method.

(37) Musaev, D. G.; Morokuma, K. *J. Chem. Phys.* **1994**, *101*, 10697.
(38) (a) Pacios, L. F.; Calzada, P. G. *Int. J. Quant. Chem.* **1988**, *34*, 267. (b) Veldkamp, A.; Frenking, G. *J. Chem. Soc., Chem. Commun.* **1992**, 118. (c) Ziegler, T.; Li, J. *Can. J. Chem.* **1994**, *72*, 783.

Downloaded by CARLI CONSORTIUM on June 30, 2009
Published on January 7, 1997 on http://pubs.acs.org | doi: 10.1021/om960601s

Table 3. Total Energies (in hartrees) of the $FeSiCH_4^+$ Isomers Computed with the TZV+P Basis Set

structure	state	CASSCF	PT2F	ω^a
$Fe^+(^6D) + H_2SiCH_2$		−1591.308 06	−1592.050 46	
$Fe^+\cdots H_2SiCH_2$ complex (**1a**)	$^6A'$	−1591.318 17	−1592.065 73	0.88
$Fe^+\cdots H_2SiCH_2$ complex (**1b**)	$^6A''$	−1591.315 47	−1592.064 01	0.88
$H_2Si-CH_2Fe^+$ open (**3a**)	$^6A'$	−1591.348 86	−1592.106 04	0.87
$H_2Si-CH_2Fe^+$ open (**3b**)	$^6A''$	−1591.347 98	−1592.105 86	0.87
$FeHSi-CH_3^+$ methyl structure (**5a**)	$^6A'$	−1591.342 33	−1592.105 53	0.87
$FeHSi-CH_3^+$ methyl structure (**5b**)	$^6A''$	−1591.343 11	−1592.106 07	0.87
TS(open → methyl structure) (**7**)	^6A	−1591.282 56	−1592.039 06	0.87
$Fe^+(^4F) + H_2SiCH_2$		−1591.247 70	−1592.050 52	
$Fe^+\cdots H_2SiCH_2$ complex (**2a**)	$^4A'$	−1591.273 27	−1592.065 34	0.84
$Fe^+\cdots H_2SiCH_2$ complex (**2b**)	$^4A''$	−1591.273 79	−1592.067 35	0.84
$(H_2Si-CH_2)Fe^+$ cyclic (**4a**)	$^4A'$	−1591.333 57	−1592.129 01	0.86
$(H_2Si-CH_2)Fe^+$ cyclic (**4b**)	$^4A''$	−1591.327 65	−1592.133 77	0.85
$FeHSi-CH_3^+$ methyl structure (**6a**)	$^4A'$	−1591.324 08	−1592.115 87	0.85
$FeHSi-CH_3^+$ methyl structure (**6b**)	$^4A''$	−1591.344 71	−1592.121 69	0.87
TS(cyclic → methyl structure) (**8**)	^4A	−1591.241 43	−1592.053 32	0.84

[a] The weight of the CASSCF reference function in the first-order wave function.[34]

Downloaded by CARLI CONSORTIUM on June 30, 2009
Published on January 7, 1997 on http://pubs.acs.org | doi: 10.1021/om960601s

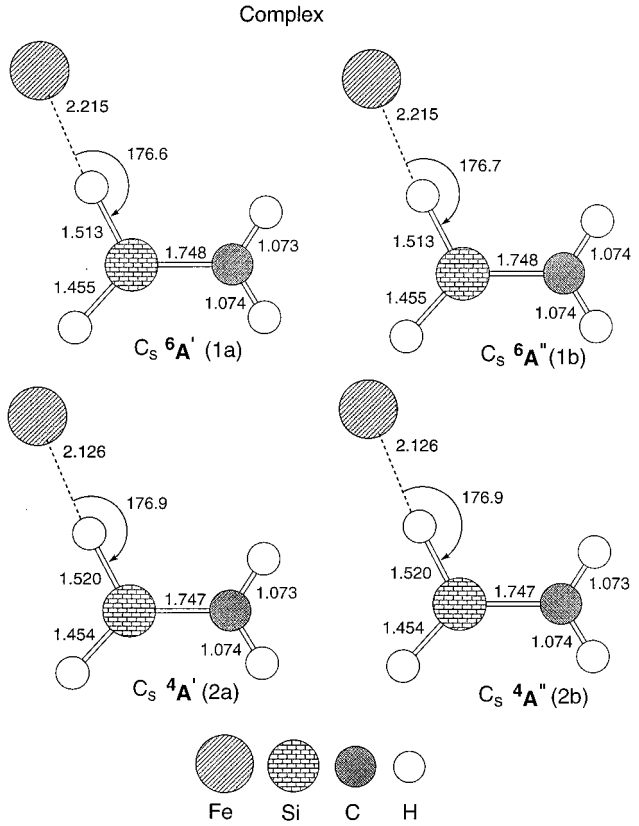

Figure 2. CASSCF (11/10) optimized geometries of the $Fe^+\cdots H_2SiCH_2$ complex for the low-lying electronic states (bond lengths in Å, bond angles in deg).

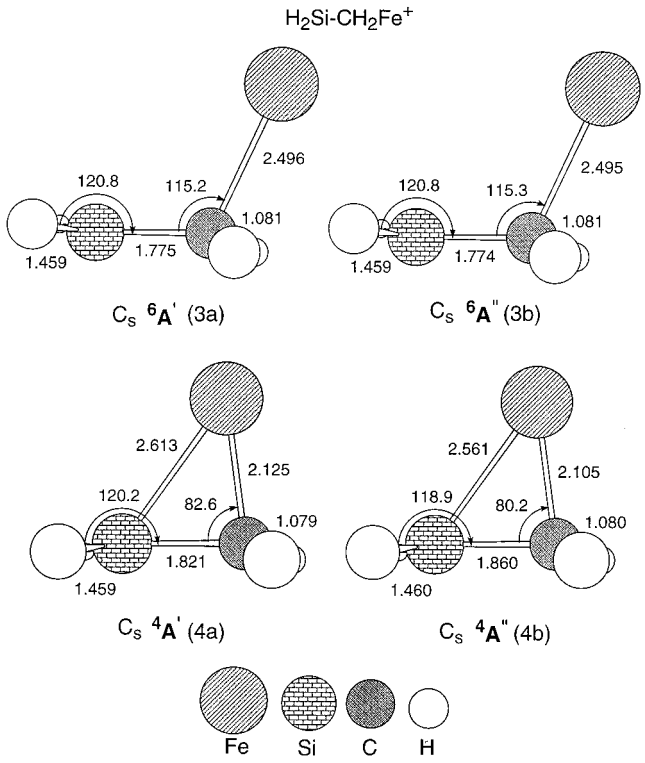

Figure 3. CASSCF (11/10) optimized geometries of the $H_2Si-CH_2Fe^+$ open and the $(H_2Si-CH_2)Fe^+$ cyclic isomers of $FeSiCH_4^+$ for the low-lying electronic states (bond lengths in Å, bond angles in deg).

much shorter than that in the open isomer, a new Si−Fe bond of 2.56−2.61 Å is formed, and the Si−C bond is lengthened significantly (by 0.07−0.11 Å) with respect to isolated silaethylene. Both quartet states of $(H_2Si-CH_2)Fe^+$ are predicted to lie appreciably lower in energy than their sextet counterparts (see below). The lowest state of cyclic $(H_2Si-CH_2)Fe^+$ is found to be $^4A''$ (**4b**), with the $^4A'$ (**4a**) state lying only 3 kcal/mol higher in energy. The $^4A''$ (**4b**) cyclic isomer is stabilized substantially with respect to isolated reactants $Fe^+(^4F)$ + H_2SiCH_2, i.e. by 52.2 kcal/mol at the CASPT2 level of theory (Table 4). For comparison, the $^6A'$ (**3a**) open isomer, which is 17.3 kcal/mol above the $^4A''$ (**4b**) cyclic one, is stabilized only by 34.9 kcal/mol relative to isolated $Fe^+(^6D)$ + H_2SiCH_2 at this level of theory.

E. Methyl Structures. A 1,2-hydrogen shift from the open isomer $H_2Si-CH_2Fe^+$ or the cyclic isomer $(H_2Si-CH_2)Fe^+$ results in the $FeHSi-CH_3^+$ isomer (Figure 4), also referred here to as a "methylstructure". This hydrogen shift is accompanied by the iron migration to the silicon end, as the carbon atom is already saturated. The $FeHSi-CH_3^+$ species can be viewed as arising from interaction of Fe^+ with the lone electron pair of methylsilylene as well. Both the Si−C and Si−H bonds of $FeHSi-CH_3^+$ are shortened (strengthened) significantly relative to those in isolated methylsilylene in all the states studied (cf. Figures 1 and 4).

As in the open/cyclic isomers, an important structural difference between the sextet $^6A'$ (**5a**) and $^6A''$ (**5b**) states and quartet $^4A'$ (**6a**) and $^4A''$ (**6b**) states of $FeHSi-CH_3^+$ is the Si−Fe distance. It decreases significantly from 2.97 Å in the sextet states to 2.32−2.51 Å in the quartet states.[32b] The CASPT2 calculations

Table 4. Relative Energies of the $FeSiCH_4^+$ Isomers and Barrier Heights for the Isomerization Reactions (in kcal/mol) Computed with the TZV+P Basis Set

structure	state	CASSCF	PT2F	exp[a]
$Fe^+(^6D) + H_2SiCH_2$		0.0	0.0	
$Fe^+\cdots H_2SiCH_2$ complex (**1a**)	$^6A'$	−6.3	−9.6	
$Fe^+\cdots H_2SiCH_2$ complex (**1b**)	$^6A''$	−4.6	−8.5	
$H_2Si-CH_2Fe^+$ open (**3a**)	$^6A'$	−25.6	−34.9	
$H_2Si-CH_2Fe^+$ open (**3b**)	$^6A''$	−25.1	−34.8	
$FeHSi-CH_3^+$ methyl structure (**5a**)	$^6A'$	−21.5	−34.6	
$FeHSi-CH_3^+$ methyl structure (**5b**)	$^6A''$	−22.0	−34.9	
TS(open → methyl structure) (**7**)	^6A	16.0	7.2	
ΔE(open → methyl structure)[b]		41.6	42.0	~40
ΔE(methyl structure → open)[c]		38.0	42.0	
$Fe^+(^4F) + H_2SiCH_2$		0.0	0.0	
$Fe^+\cdots H_2SiCH_2$ complex (**2a**)	$^4A'$	−16.0	−9.3	
$Fe^+\cdots H_2SiCH_2$ complex (**2b**)	$^4A''$	−16.4	−10.6	
$(H_2Si-CH_2)Fe^+$ cyclic (**4a**)	$^4A'$	−53.9	−49.3	
$(H_2Si-CH_2)Fe^+$ cyclic (**4b**)	$^4A''$	−50.2	−52.2	
$FeHSi-CH_3^+$ methyl structure (**6a**)	$^4A'$	−47.9	−41.0	
$FeHSi-CH_3^+$ methyl structure (**6b**)	$^4A''$	−60.9	−44.7	
TS(cyclic → methyl structure) (**8**)	^4A	3.9	−1.8	
ΔE(cyclic → methyl structure)[d]		57.8	50.5	~40
ΔE(methyl structure → cyclic)[e]		64.8	42.9	

[a] References 4 and 5. [b] The barrier to the 1,2-hydrogen shift from $H_2Si-CH_2Fe^+$ (**3a**) to $FeHSi-CH_3^+$ (**5b**). [c] The barrier to the 1,2-hydrogen shift from $FeHSi-CH_3^+$ (**5b**) to $H_2Si-CH_2Fe^+$ (**3a**). [d] The barrier to the 1,2-hydrogen shift from $(H_2Si-CH_2)Fe^+$ (**4b**) to $FeHSi-CH_3^+$ (**6b**). [e] The barrier to the 1,2-hydrogen from $FeHSi-CH_3^+$ (**6b**) to $(H_2Si-CH_2)Fe^+$ (**4b**).

Downloaded by CARLI CONSORTIUM on June 30, 2009
Published on January 7, 1997 on http://pubs.acs.org | doi: 10.1021/om960601s

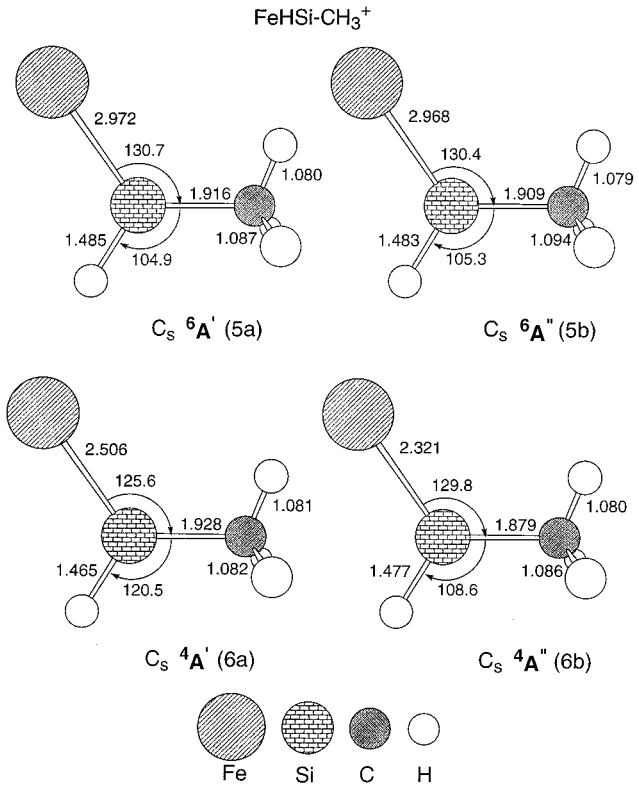

Figure 4. CASSCF (11/10) optimized geometries of the $FeHSi-CH_3^+$ methyl structure isomer of $FeSiCH_4^+$ for the low-lying electronic states (bond lengths in Å, bond angles in deg).

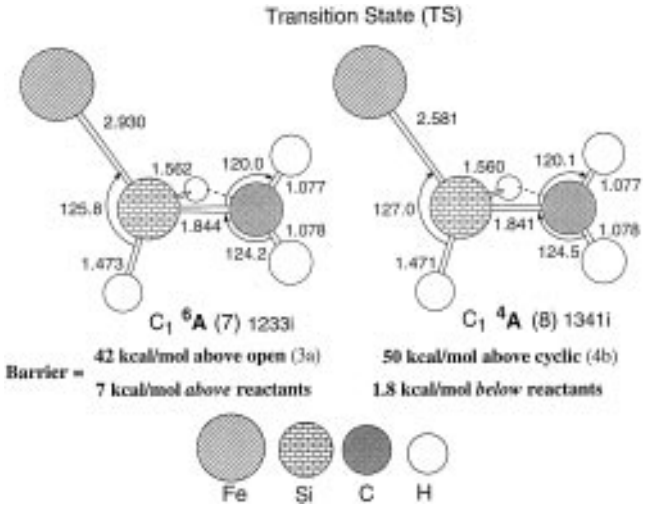

Figure 5. CASSCF (11/10) optimized geometries of the transition states for the interconversion between the open $H_2Si-CH_2Fe^+$ $^6A'$ (**3a**) and methyl structure $FeHSi-CH_3^+$ $^6A''$ (**5b**) and between cyclic $(H_2Si-CH_2)Fe^+$ $^4A''$ (4b) and methyl structure $FeHSi-CH_3^+$ $^4A''$ (**6b**) (bond lengths in Å, bond angles in deg).

predict the ground state of $FeHSi-CH_3^+$ to be a $^4A''$ (**6b**) state, consistent with its shortest Si−C (1.88 Å) and Si−Fe (2.32 Å) bond lengths among the states considered (Figure 4). The next quartet state, $^4A'$ (**6a**), is found to be only 3.7 kcal/mol higher. As in the open/cyclic isomers, both sextet states of $FeHSi-CH_3^+$ are higher in energy than the quartets; the lowest sextet state is predicted to be $^6A''$ (**5b**) located 9.8 kcal/mol above $^4A''$ (**6b**) but only 0.3 kcal/mol below the $^6A'$ (**5a**) state. $^4A''$ (**6b**) is stabilized considerably relative to isolated reactants $Fe^+(^4F) + H_2SiCH_2$, i.e. by 44.7 kcal/mol at the CASPT2 level (Table 4). On the sextet potential energy surface the stabilization is less pronounced, with $^6A''$ (**5b**) lying 34.9 kcal/mol below isolated $Fe^+(^6D) + H_2SiCH_2$.

The cyclic/open and methyl structure isomers are the most stable $FeSiCH_4^+$ isomers found in this work. We now turn to the following question: What is the barrier height to the 1,2-hydrogen migration separating them? The magnitude of this barrier is important in identification of the two distinguishable $FeSiCH_4^+$ isomers observed experimentally.[4,5]

F. Barrier between the Cyclic/Open Structure and Methyl Structure. The transition state (TS) for the interconversion between the open isomer and the methyl structure on the sextet potential energy surface, ^6A (**7**), and the TS connecting the cyclic isomer with the

methyl structure on the quartet surface, ^4A (**8**), are depicted in Figure 5. In the two TS's of no symmetry, both the hydrogen being transferred and iron are at the silicon end. Thus, the H and Fe migrations appear to be asynchronous (cf. Figures 4 and 5). Once more the quartet structure (**8**) shows a much shorter Si−Fe bond length (2.58 Å) than the sextet structure (**7**) (2.93 Å).

The ^6A TS (**7**) is predicted to lie 7.2 kcal/mol above the $Fe^+(^6D) + H_2SiCH_2$ reactants at the CASPT2 level, indicating that there is a net barrier for the reaction on the sextet potential surface. The ^6A TS (**7**) is found to be 42.0 kcal/mol above the open $^6A'$ (**3a**) isomer. In contrast, on the quartet surface, the ^4A TS (**8**) is found to be 1.8 kcal/mol *below* the $Fe^+(^4F) + H_2SiCH_2$ reactants, suggesting no net barrier for the reaction. The CASPT2 barrier height for the cyclic $^4A''$ (**4b**) → methyl structure $^4A''$ (**6b**) interconversion via the ^4A TS (**8**) of 50.5 kcal/mol is 8.5 kcal/mol higher than that for the corresponding rearrangement on the sextet surface (see Table 4 and Figure 5). Both interconversion barrier heights are of the order of magnitude of that predicted for the silaethylene → methylsilylene isomerization[24f,g,h,29] and correspond nicely with the experimental estimate for the [$FeCSiH_4$+] isomerization barrier.[4,5]

IV. Conclusions

The open $H_2Si-CH_2Fe^+$ $^6A'$ (**3a**)/cyclic (H_2Si-CH_2)-Fe^+ $^4A''$ (**4b**) and the methyl structure $FeHSi-CH_3^+$ $^6A''$ (**5b**) and $FeHSi-CH_3^+$ $^4A''$ (**6b**) isomers are predicted here to be the most stable $FeSiCH_4^+$ isomers.[36] These are therefore the most likely candidates for the two distinguishable $FeSiCH_4^+$ species observed in the gas-phase mass-spectrometric experiments.[4,5] This conclusion is strongly supported by the computed barriers (42−50 kcal/mol) separating the relevant pairs of the $FeSiCH_4^+$ isomers. The magnitude of the barriers is consistent with the experimental estimate. On the quartet surface the net isomerization barrier (relative to separated reactants) is zero, whereas there is a net 7.2 kcal/mol barrier on the higher energy sextet surface. This suggests that the reaction dynamics, especially as it relates to the efficiency of intramolecular vibrational energy transfer into the isomerization coordinate, plays an important role in the observation that the two isomers do not interconvert at thermal energies.

Acknowledgment. The authors thank Professor D. B. Jacobson for sending us preprints of his work. We also acknowledge enlightening discussions with Drs. M. W. Schmidt, N. Matsunaga, and K. A. Nguyen. This work was supported in part by grants from the Air Force Office of Scientific Research (No. F49620-95-1-0073) and the National Science Foundation (CHE-9313717).

OM960601S

Downloaded by CARLI CONSORTIUM on June 30, 2009
Published on January 7, 1997 on http://pubs.acs.org | doi: 10.1021/om960601s